ORIGINAL RESEARCH

The Idiosyncratic Efficacy of Spironolactone-Loaded PLGA Nanoparticles Against Murine Intestinal Schistosomiasis

Walaa Ebrahim Abd El Hady [iD][1], Ghada Ahmed El-Emam [iD][1], Nora E Saleh[2], Marwa M Hamouda[2], Amira Motawea [iD][1]

[1]Department of Pharmaceutics, Faculty of Pharmacy, Mansoura University, Mansoura, Egypt; [2]Department of Medical Parasitology, Faculty of Medicine, Mansoura University, Mansoura, Egypt

Correspondence: Amira Motawea, Email a_metawea@mans.edu.eg

Background: Schistosomiasis is a chronic debilitating parasitic disease accompanied with severe mortality rates. Although praziquantel (PZQ) acts as the sole drug for the management of this disease, it has many limitations that restrict the use of this treatment approach. Repurposing of spironolactone (SPL) and nanomedicine represents a promising approach to improve anti-schistosomal therapy. We have developed SPL-loaded poly(lactic-co-glycolic acid) (PLGA) nanoparticles (NPs) to enhance the solubility, efficacy, and drug delivery and hence decrease the frequency of administration, which is of great clinical value.

Methods: The physico-chemical assessment was performed starting with particle size analysis and confirmed using TEM, FT-IR, DSC, and XRD. The antischistosomal effect of the SPL-loaded PLGA NPs against *Schistosoma mansoni* (*S. mansoni*)-induced infection in mice was also estimated.

Results: Our results manifested that the optimized prepared NPs had particle size of 238.00 ± 7.21 nm, and the zeta potential was -19.66 ± 0.98 nm, effective encapsulation $90.43 \pm 8.81\%$. Other physico-chemical features emphasized that nanoparticles were completely encapsulated inside the polymer matrix. The in vitro dissolution studies revealed that SPL-loaded PLGA NPs showed sustained biphasic release pattern and followed Korsmeyer–Peppas kinetics corresponding to Fickian diffusion ($n<0.45$). The used regimen was efficient against *S. mansoni* infection and induced significant reduction in spleen, liver indices, and total worm count ($\rho<0.05$). Besides, when targeting the adult stages, it induced decline in the hepatic egg load and the small intestinal egg load by 57.75% and 54.17%, respectively, when compared to the control group. SPL-loaded PLGA NPs caused extensive damage to adult worms on tegument and suckers, leading to the death of the parasites in less time, plus marked improvement in liver pathology.

Conclusion: Collectively, these findings provided proof-of-evidence that the developed SPL-loaded PLGA NPs could be potentially used as a promising candidate for new antischistosomal drug development.

Keywords: spironolactone, poly (lactic-co-glycolic acid), nanoparticles, *Schistosoma mansoni*, egg load, oogram

Introduction

In many developing countries, schistosomiasis, a parasitic disease caused by the blood flukes *Schistosoma*, still represents an endemic severe disease that has severe social and economic implications.[1] It affects around 240 million people worldwide, with over 750 million living in locations where the parasite is endemic.[2] In terms of mortality and morbidity, the World Health Organization's Tropical Diseases Research division identifies schistosomiasis as the primary neglected tropical helminthic disease and showed that at least 236.6 million people required preventive treatment in 2019. Schistosomiasis transmission has been reported from 78 countries as it is considered common in tropical and subtropical regions, particularly in underdeveloped populations without access to clean water and proper sanitary facilities.[3] In Africa, the Near East, and South America, the parasite *Schistosoma mansoni* causes intestinal schistosomiasis, which affects roughly 80 million people in these locations. *Schistosoma* eggs trapped in the tissues are the main pathogenic causative agents. The prolonged inflammatory response to these eggs causes periportal fibrosis, coupled with

987

portal hypertension and all its sequels of ascites, hematemesis, and melena in advanced instances.[4] Due to the lack of a vaccine, the schistosomiasis control approach focuses on limiting morbidity by frequent treatment with praziquantel (PZQ). Praziquantel is presently the sole commercially used and approved treatment for schistosomal infections despite schistosomiasis being a global disease. Although PZQ shows great effectiveness against all *Schistosoma* species that affect humans, it also has a number of drawbacks, including an incomplete effectiveness profile, poor pharmacokinetics, and an unpleasant taste, all of which may restrict attempts of complete eradication of the disease.[5] The lack of full cures in PZQ-treated populations may be related to the drug's inadequate long-lasting effects and limited absorption, which are attributable to its hydrophobic nature, so it was formulated as solid lipid nanoparticles (SLNs) to overcome these difficulties.[6] As reported by Amara et al,[7] for more proficient PZQ mass chemotherapy, PZQ-lipid nanocarriers may be a tolerable single oral nanomedicine dosage. Moreover, one of the most important drawbacks of PZQ is its poor effectiveness toward the immature stages. In other words, PZQ has been used as a treatment for only the adult stages for more than three decades. Thus, the development of PZQ-resistant *Schistosoma* strains represents the largest challenge for work in that field, especially with identification of resistance both experimentally and in the field. Therefore, the discovery of novel antischistosomal drugs is a convincing goal for these reasons, and several lines of research are carried out either using newly synthesized drugs or toward discovering the antischistosomal abilities of present medications. Although there is an ongoing demand for safe and cost-effective pharmaceuticals that can be used in resource-poor areas, developing new drugs is a time-consuming and expensive process. Tragically, a lot of pharmaceutical firms have scaled back their attempts to create new drugs.[8] Recent developments in nanomedicine (including chemotherapeutic agents, biological agents, immunotherapeutic agents, etc.) for the treatment of various diseases have produced a number of unresolved applications.[9] Nanotechnology has completely changed the drug delivery and targeting industries due to its extraordinary properties, including tiny particle size, large exposed surface area, increased physical and chemical stability, and high biocompatibility of its constituents. Furthermore, independently of the physical characteristics of a medicine, nanotechnology can enhance the solubility, dissolution, permeability, and bioavailability of that drug.[10] Drug repositioning or re-profiling (finding new indications for existing drugs) might be a potential technique for speeding up drug development and discovery in the fight against schistosomiasis. Several researches have tested numerous therapeutic medications that have been licensed by the US Food and Drug Administration or its international equivalents in recent years against *S. mansoni* adult worms, and discovered many prospective compounds.[11–13] Diuretics are the most widely recommended medicine class for fluid congestion alleviation, particularly in patients with heart failure, renal failure, or liver cirrhosis. Owing to their excellent pharmacokinetics, such as their reasonable safety, oral administration, tolerability, and inexpensiveness, researchers were motivated to explore their antischistosomal abilities against *S. mansoni* ex vivo using a phenotypic drug screening technique. Spironolactone, the potassium-sparing diuretic, proved significant antischistosomal properties as the microscopic investigations of adult parasite showed effects on movement and shape of schistosomes at various drug doses, dramatically decreased worm load, egg production, and hepatosplenomegaly in experimentally infected mice, showing the diuretic's potential usefulness as an antischistosomal medication with therapeutic repurposing.[4] New medication development is a protracted slow-moving process with significant attrition rates and significant expenditures; successfully bringing them to market requires more work. In fact, the early stages of clinical trials for therapeutic candidates typically result in their failure due to toxicity or ineffectiveness, besides the lengthy procedure necessary in getting them to market, which is expected to take between 10 and 17 years.[14] In this context, pharmaceutical business and the research community are becoming more and more interested in drug repositioning, also known as drug repurposing. This strategy seeks to shorten the timeline, expense, and risk of conventional drug development, while also identifying new therapeutic possibilities for medicines already on the market.[15] Hence, examples of successfully repositioned nano-based drugs include niclosamide-nanostructured lipid carriers[14] and Guanabenz acetate- nanopolymersomes[16] for treatment of cancer diseases. Spironolactone, a potassium-sparing diuretic, is a mineralocorticoid receptor antagonist that targets aldosterone specifically,[17,18] and it is a highly successful medication for the treatment of heart failure,[19] myocardial infarction,[20] and resistant hypertension.[21] Spironolactone was also utilized in the treatment of resistant ascites accompanying schistosome liver disease, in combination with a short-term course of corticosteroids. Spironolactone was also beneficial in alleviating respiratory distress in a case of myocarditis caused by malarial infection.[22] Based on several reviews of the literature on new advancements in oral administration, we

revealed that PLGA nanoparticles showed promise in increasing drug stability across the GIT, as well as other advantages of nanocarrier systems, all of which can contribute to increased oral bioavailability.

Poly(lactic-co-glycolic acid) (PLGA) is one of the most often adopted polymers in the design and formulation of drug delivery systems for biomedical applications because of its biodegradability, biosafety, biocompatibility, variety in formulation, and functionalization, and it is also an FDA-approved copolymer.[23] PLGA-based nanocarriers protect the encapsulated medication against premature breakdown in the biological fluid, ensuring excellent bioavailability,[24] delivering a prolonged (tunable degradation kinetics) and targeted administration, enhancing bioactive ingredient intracellular penetration, and decreasing adverse effects. In vivo, polymeric NPs can be destroyed by enzymes, hydrolysis, or both, to yield biocompatible, toxicologically harmless by-products that are later eliminated by normal metabolic routes.[25] Among the applied techniques for preparing PLGA-based NPs, the single emulsion solvent evaporation method was found to be the most preferable one,[26] which has been efficiently suited for encapsulating water-insoluble drugs such as steroids.[27] Several modifications have been developed over the years to improve the results obtained with this technique. The aim of this study was to develop, characterize, and optimize a polymeric nanoparticulate delivery system of spironolactone with the biocompatible and degradable PLGA. Additionally, the antischistosomal activity of the selected spironolactone-loaded PLGA nanoparticles was assessed in mice that had been experimentally infected with *S. mansoni*.

Materials and Methods
Materials
Spironolactone (SPL) was obtained from Sigma-Aldrich, St. Louis, MO, USA. Poly(lactic-co-glycolic acid) (PLGA) (lactide–glycolide 50:50 (ester terminated) and 75:25 (acid terminated), Viscosity 1 and 0.2 dL/g, respectively) was kindly supplied by Purac Biomaterials, Holland. Polyvinyl alcohol (87.0–89.0% hydrolyzed, molecular weight 31,000–50,000 Da) was obtained from Acros Organics, Belgium. Acetone, methylene chloride, dimethylsulfoxide (DMSO), and methanol were bought from Adwic, EL Nasr Pharmaceutical Chemicals, Co., Egypt. All other materials were of fine analytical grades. Praziquantel (PZQ) was supplied from Alexandria Company for Pharmaceuticals & Chemical Industries, Egypt.

Preparation of SPL NPs
The effects of various formulation parameters including PLGA type, PLGA amount, the organic phase type on the particle size, entrapment efficiency% (EE%), and zeta potential of SPL NPs were studied to select the optimum formula (Table 1). Two different types of PLGA with a ratio of lactide:glycolide 50:50 and 75:25 were used at the amount of 50 mg or 100 mg. The organic solvents used were acetone and methylene chloride (DCM) individually as they are good

Table 1 Characterization of the Prepared Nanoparticles, Each Formula Containing 25 mg Drug

Formula Code	Polymer Type	Polymer (mg)	Solvent Type	Size (nm)*	PDI*	EE%*	Zeta Potential*
F1	PLGA 75:25	50	Acetone	323.5±25.17	0.20±0.01	74.30±2.40	−30.20±4.51
F2		100		290.36±15.34	0.27±0.07	89.36±3.37	−24.73±0.20
F3		50	DCM	252.26±2.81	0.08±0.04	66.10±5.73	−16.76±0.11
F4		100		238.00±7.21	0.06±0.00	90.43±8.81	−19.66±0.98
F5	PLGA 50:50	50	Acetone	401.55±25.95	0.40±0.02	76.70±6.45	−23.23±1.04
F6		100		352.75±43.06	0.48±0.02	84.75±7.19	−15.30±0.34
F7		50	DCM	294.00±5.65	0.09±0.03	71.30±1.69	−12.15±0.21
F8		100		267.56±8.46	0.14±0.03	90.32±4.55	−12.46±0.49

Note: *Data are expressed as mean ± SD (*n*=3).

solvents for PLGA and much less toxic than other solvents such as chloroform and acetonitrile.[28] Nanoparticles loaded with SPL were prepared according to the type of solvent by nanoprecipitation method if acetone was used[29] and emulsion solvent evaporation technique when DCM was used.[26,30]

Briefly, accurately weighed PLGA and SPL (25 mg) were dissolved in 3 mL of either acetone or DCM using a vortex mixer (Model VM-300, Gemmy Industrial Corp, Taipei, Taiwan) (Table 1). Under ultrasonic homogenization (Ultrasonic homogenizer, Cole-Parmer Instrument Co., Chicago, Illinois, USA) at 90% amplitude, the organic phase was injected slowly to 15 mL aqueous phase containing 2% w/v polyvinyl alcohol (PVA). The organic solvent was evaporated overnight under moderate magnetic stirring (Heidolph, Illinois, USA). NPs were collected after centrifugation at 13,000 rpm (15,100×g) (Heraeus, GmbH, Osterode, Germany) for 1 h and washed three times with deionized water. The recovered NPs were resuspended in deionized water and freeze-dried (SIM, FD8-8T, Newark, NJ, USA).

Characterization of SPL NPs

Determination of Drug Entrapment Efficiency% (EE%)

The freeze-dried NPs were dissolved in 10 mL DMSO and adequately diluted with methanol to be measured spectrophotometrically at 244 nm (ultraviolet/visible [UV/VIS] spectrophotometer; JASCO, Tokyo, Japan) against a blank of plain NPs prepared in the same way. The tests were carried out in triplicate. The entrapment efficiency (EE%) was calculated using the following equation:[31,32]

$$EE \% = \frac{\text{mass of drug in NPs}}{\text{mass of drug added}} \times 100$$

Particle Size Analysis and Polydispersity Index (PDI)

The size distribution and PDI of the prepared SPL NPs were assessed using dynamic light scattering (Malvern Instruments, Malvern, UK). Samples were properly diluted 10 times with deionized water and measured in triplicate.[10]

Zeta Potential Determination

To determine the zeta potential, the properly diluted samples of the prepared SPL NPs (ratio 1:10) were placed in an electrophoretic cell, then measured using a photon correlation spectroscopy-based instrument at 25 °C (Malvern Instruments, Malvern, UK) to determine NPs' surface charge.[10]

Surface Morphology

A drop of the optimized nanoparticle dispersion (F4) was deposed onto a formvar/carbon tape covered by a copper grid prior to examination by transmission electron microscopy (TEM, JEM-1230, JOEL, Japan). Excess dispersion was eliminated by a tip of filter paper, and the samples were allowed to dry at room temperature. The images were then visualized via the TEM microscope at 120 kV with different magnifications using iTEM software.[33]

Fourier Transform Infrared Spectroscopy

The FTIR spectra are mostly used to appraise the state and any chemical interaction between the drug and excipients. This technique applies extensive information about the functional group exhibited in a formulation.[33] FT-IR spectra of SPL, PLGA, physical mixture (PM) of SPL, PLGA+PVA, plain F4, and SPL-loaded PLGA (F4) were scanned with Cary 630 FTIR Spectrometer (Thermo Fisher Scientific, Inc., Waltham, MA, USA) employing the KBr disk method. Each sample (about 2 mg) was blended with KBr and transformed into a pellet. The spectra were scanned in the frequency range of 4000–400 cm^{-1} at a spectral resolution of 4 cm^{-1}.

Thermal Analysis

Differential scanning calorimetry (DSC) identifies the crystalline besides the amorphous behavior of the drug in nanoparticles via monitoring the temperature and heat flow combined with thermal transitions in a formulation.[33] DSC curves of pure SPL, polymer (PLGA), PM, and the prepared nanoparticles (plain and the corresponding medicated F4) were performed by differential scanning calorimeter (Pyris 6 DSC, Perkin Elmer, USA). Thermal scans were documented by heating each sample (5 mg) in an aluminum Tzero pan from 30 to 300 °C at a heating rate of 10 °C/min under

a constant flow of nitrogen at 20 mL/min and cooling back to 30 °C at the same rate. An empty aluminum pan was taken as a reference, and the device was standardized with indium (99.9% pure calibration standard). The midpoint of the onset and end set temperature was represented by the glass transition temperature of the sample.[34]

X-Ray Diffraction

The X-ray diffraction (XRD) pattern was investigated to obtain the information involving physical state identification and crystal lattice arrangement. The crystalline behavior of SPL, PLGA, PM, plain, and medicated F4 was examined by XRD (Bruker D8 Advance, Germany) via placing a sample on a zero-background aluminum holder plate, using a Cu Kα source (40 mA, λ = 1.542 Å, 40 kV). Data were collected and analyzed with 2θ scan range of 3–45° at a scanning rate of 10° min^{-1} in a uniform scan mode at room temperature.[33]

In vitro Dissolution Study

The in vitro dissolution study of SPL from the optimized PLGA NPs compared to free SPL was conducted by following the protocol of the USP apparatus II (paddle method) (Dissolution Apparatus USP Standards, Scientific, DA-6D, Bombay, India).[30,35] Accurately weighed samples of the freeze-dried SPL NPs equivalent to 10 mg drug were added to the vessels containing 500 mL of 0.1N HCl (pH 1.2) or 0.066M phosphate buffer (pH 6.8) with paddle rotation speed of 100 rpm at 37 ±0.5 °C. At different time intervals (0.25, 0.5, 1, 1.5, 2, 3, 4, 6, 12, and 24 h), 3 mL of the dissolution medium were withdrawn and replaced with an equivalent volume of the fresh medium. The collected samples were filtered and analyzed spectro-photometrically for drug amount at 242 nm against the blank of plain NPs treated the same (ultraviolet/visible [UV/VIS] spectrophotometer; JASCO, Tokyo, Japan). The experiments were performed three times, and the average drug release % was calculated at each time interval and plotted against time to construct the in vitro dissolution curves.

Release Kinetics

To describe the release kinetics of SPL from the prepared NPs, mathematical models were used. The release data were fitted to models representing zero-order, first-order,[36] as well as diffusion-controlled release model.[37] The Korsmayer–Peppas kinetic model ($M_t/M_\infty = k_p t^n$) was also utilized as a logarithmic relationship of the proportion of drug released (M_t/M_∞) after time (t) to evaluate the release mechanism.[38] The model with the highest correlation coefficient (r^2) was suggested to describe the drug release mechanism from the investigated NPs.

In vivo Assessment of Antischistosomal Abilities of Treatment Regimens on Mice Models

Parasites and Infection

Nearly 40 laboratory-bred Swiss albino female mice (CD-I strain, aged 6–8 weeks, and weighing 20–25 g) were used in this study. Mice were subcutaneously infected with *S. mansoni* cercariae (80 ± 10 cercariae), that shed from infected *Biomphalaria alexandrina* snails. All animal studies were approved by the Medical Experimental Research Center (MERC), Faculty of Medicine, Mansoura University, Mansoura, Egypt, based on the institutional and national regulations for animal experimentation and IRP approval (R.21.8.1400). Studies were conducted in accordance with the "Declaration of Helsinki, the Guiding Principle in Care and Use of Animals" (DHEW publication NIH 80–23), and the "Principles of Laboratory Animal Care" (NIH publication #85–23, revised in 1985). Infected mice were kept in an air-conditioned animal house, at 20–22 °C, with 12 h light and 12 h dark cycle, and maintained on a standard commercial pellet diet, and normal drinking water *ad libitum*.

Animal Groups

Mice were randomly divided between five groups:

Group I: infected non-treated (*n* = 8).
Group II: infected and treated with PZQ in the 6th week post infection (*n* = 6).
Group III: infected and treated with plain F4 in the 6th week post infection (*n* = 6).
Group IV: infected and treated with SPL in 6th week post infection (*n* = 10).
Group V: infected and treated with F4 in 6th week post infection (*n* = 10).

The treatment was given in the 6th WPI as indicated previously. Later, mice of all groups were euthanized at 9 WPI using intraperitoneal injection of 100 mg/kg of sodium thiopental.

Parasitological Assessment of Infection

Following euthanasia, the effect of used drug regimens was assessed through the following parameters:

- Liver and spleen indices: Liver and spleen were removed and weighed to assess the ratio of liver or spleen to the total mouse body weight as an indicator for the hepatosplenomegaly associated with infection.
- Adult worm burden: Perfusion of the porto-mesentric vessel was done using 0.9% saline and 0.45% sodium citrate. The revealed worms were separated and counted.[39]
- Tissue egg load:[40] Parts of intestine and liver tissue were weighed and digested with 4% KOH overnight at room temperature. The eggs were counted in at least three aliquots of 10 μL each from the suspension, and the number of eggs per suspension was determined using a light microscope. Then the tissue egg burden per gram of tissue was mathematically calculated.
- Oogram pattern:[41] One centimeter parts of the small intestine were washed and pressed between slides. Approximately 100 eggs were evaluated with regard to their stage of development (immature, mature, and dead).

Scanning Electron Microscopy Studies

Adult worms obtained from portal-mesenteric veins perfusion were washed then fixed in glutaraldehyde phosphate in order to be processed for examination using scanning electron microscopy (SEM, JEOL, JSM-6510LV, USA) in Electron Microscopy Unit, Faculty of Agriculture, Mansoura University.

Histopathological Study

Liver portions from euthanized mice were fixed in 10% formalin and processed to paraffin blocks. Sections were cut (5 μm thick) and then stained with hematoxylin and eosin (H+E). Liver sections were examined under a low-power lens of a light microscope to study histopathological changes in liver tissue, granuloma formation, and other pathological changes.[42]

Statistical Analysis

GraphPad Prism version 5.00 (GraphPad software, San Diego, CA, USA) was used for statistical analysis using one-way analysis of variance (ANOVA), followed by Tukey–Kramer multiple comparisons test. The data from all experiments were expressed as the mean value ± SD. The statistical differences at $\rho < 0.05$ were considered significant.

Results and Discussion

Characterization of SPL NPs

PLGA NPs were prepared by two methods: emulsion solvent evaporation, in which the polymer was dissolved in DCM as water immiscible volatile organic solvent; and nanoprecipitation method, where acetone was used as semi-polar, volatile, and water-miscible organic solvent. The interfacial deposition of a polymer into the aqueous medium after rapid diffusion of the organic solvent is the basis of the nanoprecipitation method.[43] The most critical factors affecting NPs particle size prepared by nanoprecipitation were the concentration and viscosity of the organic phase,[44] while with the emulsion solvent evaporation method the homogenization speed as well as the concentration and type of the polymer influenced the NPs particle size.[45]

Entrapment Efficiency (EE%)

The EE% of SPL NPs formulations was found to be 66.10±5.73% to 90.43±8.81% (Table 1). The preparation method has no statistically significant effect ($\rho < 0.05$) on the entrapment of SPL in PLGA.[43]

The results showed that the polymer amount effect on EE% was more pronounced than the effect of polymer type and organic phase nature (Table 1). When the polymer amount was increased from 50 to 100 mg, the EE% increased. As the

amount of the polymer increased, the organic phase viscosity elevated, providing an additional barrier against the drug diffusion from the organic phase to the aqueous one.[46] Also, the high drug entrapment may be attributed to the attraction of free drug molecules within the matrix of polymer towards those in the aqueous phase.[30]

Particle Size Analysis

Particle size of all prepared SPL NPs formulations was ≤401.55±25.95 nm, and PDI values were ≤0.48±0.02, providing narrow size distribution. The effects of both polymer type and amount as well as the nature of the organic phase on the particle size were investigated (Table 1).

The average particle size insignificantly decreased when the amount of PLGA increased from 50 to 100 mg for both types ($\rho<0.05$). This led to slight increasing in organic phase viscosity which might have counteracted the diffusion and Ostwald ripening that inhibits large particles' growth over that of smaller ones.[30,47,48] So, the particle size decreased with employing the high PLGA amount (100 mg).

SPL NPs produced with PLGA 75:25 (F1-F4) showed a smaller particle size than those produced with PLGA 50:50 (F5-F8) at the same polymer amount. The carboxylic acid-terminated polymer (PLGA 75:25) is more hydrophilic than the ester-terminated one (PLGA 50:50) with improved polymer–water interactions, decreasing the contact angle and enhancing interfacial tension; this could end up in smaller NPs.[49]

When the emulsion solvent evaporation technique was employed, a smaller size of SPL NPs was produced compared to those obtained using nanoprecipitation method ($\rho<0.05$).[43] DCM is a superior organic solvent for PLGA and has a lower solubility in the aqueous phase as well as higher volatility than acetone, encouraging its evaporation at short time even when magnetic stirring is used at normal atmospheric pressure.[50] Solvent evaporation precludes the coalescence and agglomeration of the NPs, which results in smaller NPs.[51,52]

Zeta Potential

Table 1 shows that zeta potential of SPL NP formulations was found to be in the range of −12.15±0.21 to −30.20±4.51. There was a considerable difference ($\rho<0.05$) in zeta potential results between the formulations with PLGA 75:25 and PLGA 50:50. It is due to the polymer termination groups, which are acid- and ester-terminated, respectively.[53] In other words, zeta potential of SPL NPs prepared using PLGA 75:25 was higher than in those prepared using PLGA 50:50 due to acid termination. The high zeta potential values of SPL NPs can result in a greater repulsive force, implying more stability against aggregation.[54] The highest EE%, as well as the lowest particle size and PDI, was obtained in F4 which was selected to be further investigated compared to the free drug (Figure 1A and 1B).

TEM showed that the selected NPs were smooth, spherical in shape, homogeneously distributed, and with uniform density. The mean particle size was about 150 nm (Figure 1C), which was somewhat smaller than the DLS results due to the hydration layer formed around the PLGA NPs.[55] It shows that the solvent is attached well to the thin electric dipole layer surface when a particle passes through a liquid medium in the case of DLS analysis. Consequently, this layer affects particle motion in the environment. Thus, the hydrodynamic diameter provides data about the nanoparticle under the effect of Brownian movement, together with any coating material and a solvent layer adhered to the particle. In contrast, this hydration layer is not available, and only the information about the particle is obtained in the case of TEM analysis.

Fourier Transform Infrared Spectroscopy (FT-IR)

The schematic representation of the FT-IR spectrum is illustrated in Figure 2A. The SPL spectra revealed distinct peaks at 2952 cm^{-1} and 1769 cm^{-1} indicative of the alkane, and aromatic C-H stretching groups, respectively. The conspicuous peak at 1690 cm^{-1} is owing to stretching of imine/oxime C=N. The existence of sulfonate S=O stretching was verified by the distinctive peak at 1189 cm^{-1}, while the feature's peak revealed the halo complex C-Br stretch group at 638 cm^{-1} (Figure 2A(i)).[56] The presence of PLGA was confirmed at 1751 cm^{-1} due to stretching of C=O carboxylic.[57] Additionally, 1190 cm^{-1} was assigned to the C–N group, CH$_3$ group present at 1459 cm^{-1}, and 1626 cm^{-1} was attributed to N–H stretching vibrations of the NH group. Meanwhile, peaks at 1090–1133 cm^{-1} comprise the ester group (mainly C–O band) which is linked with water and undergoes PLGA hydrolysis, hence ensuring a sustained release of SPL from nanoparticles (Figure 2A(ii)). As elucidated in Figure 2A(iii–v), all of the drug's characteristic peaks can be found in the PM spectra at the same wavenumber, indicating that there is no chemical incompatibility or interaction between the drug
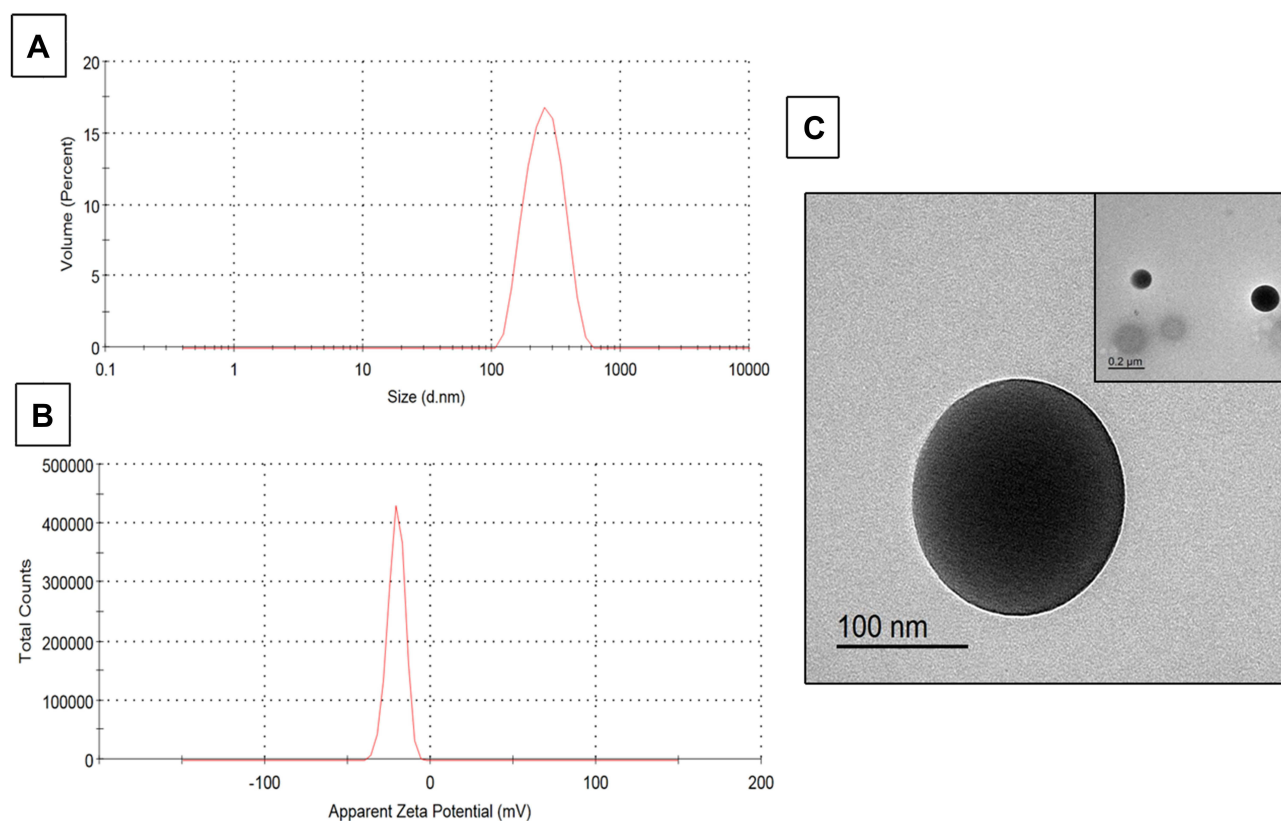
Figure 1 Particle size, zeta potential distribution curves, and TEM images for optimized SPL-NPs (f4). Particle size distribution curve (**A**), zeta potential distribution curve (**B**), TEM image (**C**).
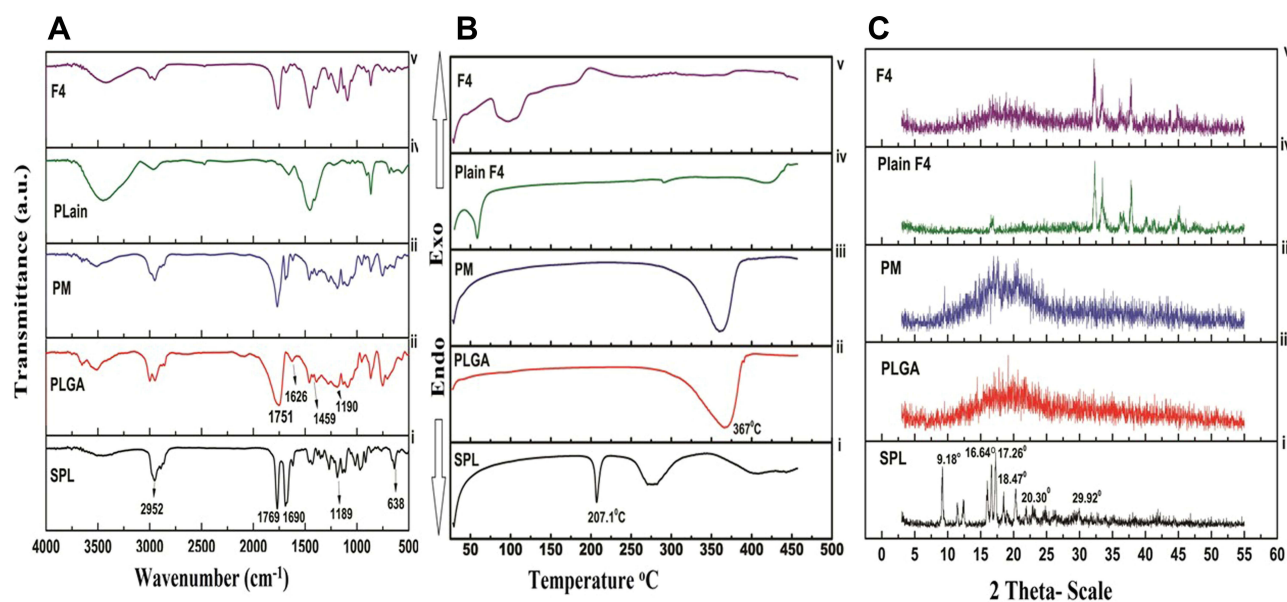

Figure 2 Fourier transform infrared (**A**), Differential scanning calorimetric (**B**) thermograms, and X-ray diffraction (**C**) spectra of (i) pure SPL, (ii) PLGA, (iii) physical mixture of SPL-PLGA-PVA (PM), (iv) plain F4, and (v) medicated F4.

and the excipients.[55] As shown in Figure 2A(v), some characteristic peaks of the drug in the nanoparticles may be diminished or disappear due to encapsulation and/or weak absorption of SPL within the polymeric network.[58]

Physical Characterization of SPL-Loaded PLGA Nanoparticles

The physical state of the drug in the prepared nanoparticles was investigated using DSC and XRD techniques (Figure 2B and C). As depicted in Figure 2B(i), the melting of crystalline SPL appears on the DSC thermograms at 207 °C. Any other peaks noticed belong to water loss, decomposition (as a characteristic degradation form of PLGA with peaks near 367 °C in Figure 2B(ii)), or evaporation above the melting point. Meanwhile, the sharp peak revealed that the drug was in a crystalline state as detected in the pure SPL and PM (Figure 2B(i) and (iii)). Surprisingly, the vanishing of melting peaks instead of the intense steep peak of SPL plus the broadening peak of the PLGA polymer in F4 further suggested that SPL was incorporated into the polymer matrix. In other words, the drug exists in an amorphous or partially crystalline state as mentioned in Figure 2B(v). Also, this study affirms the drug presence in a solubilized form in the lipid due to solid-state interaction generated by heating.

The XRD measurement also identified distinct characteristic patterns for all crystalline materials. As demonstrated in Figure 2C(i), the diffraction pattern of SPL showed different intense peaks at 9.18°, 16.64°, 17.26°, 18.47°, 20.30°, and 29.92°, mirroring its crystalline nature. Although PLGA was amorphous, the signs of crystalline drug were still detectable in the physical mixture revealing the ability of these processes to pinpoint crystallinity in amorphous matrices even at low concentration as shown in Figure 2C(ii–iii). These characteristic peaks were absent in F4 spectra like their respective plain as shown in Figure 2C(iv–v), reflecting its structural modification from a crystalline to an amorphous form of the drug. In the light of all FTIR, DSC, XRD data, it can be revealed that SPL-loaded PLGA nanoparticles were successfully prepared and completely dispersed/encapsulated inside the polymer matrix.[58]

In vitro Dissolution Study

Dissolution profiles of SPL from the optimized PLGA NPs (F4) compared to free drug suspension are depicted in Figure 3. SPL is a poorly soluble class II drug with hydrophobic properties and limited surface area available for dissolution.[59] SPL maximum dissolution was 38.27±3.67% in 0.1N HCl and 46.0±2.35% in 0.066M phosphate buffer after 3 h. In contrast, PLGA NPs showed a significant increase in the drug dissolution (about 63–75% after 8 h) in both media ($\rho < 0.05$), and this persisted in a controlled manner up to 24 h. Based on the Noyes–Whitney equation, drug dissolution is directly proportional to the surface area of drug available for dissolution. The reduced particle size provided a large surface area.[60,61] Also, the drug entrapped in NPs was found in an amorphous state as depicted by DSC and XRD data. Accordingly, the increase in dissolution profile between free drug and SPL NPs could be ascribed to both of these variables (size and the particles' solid state).[62]
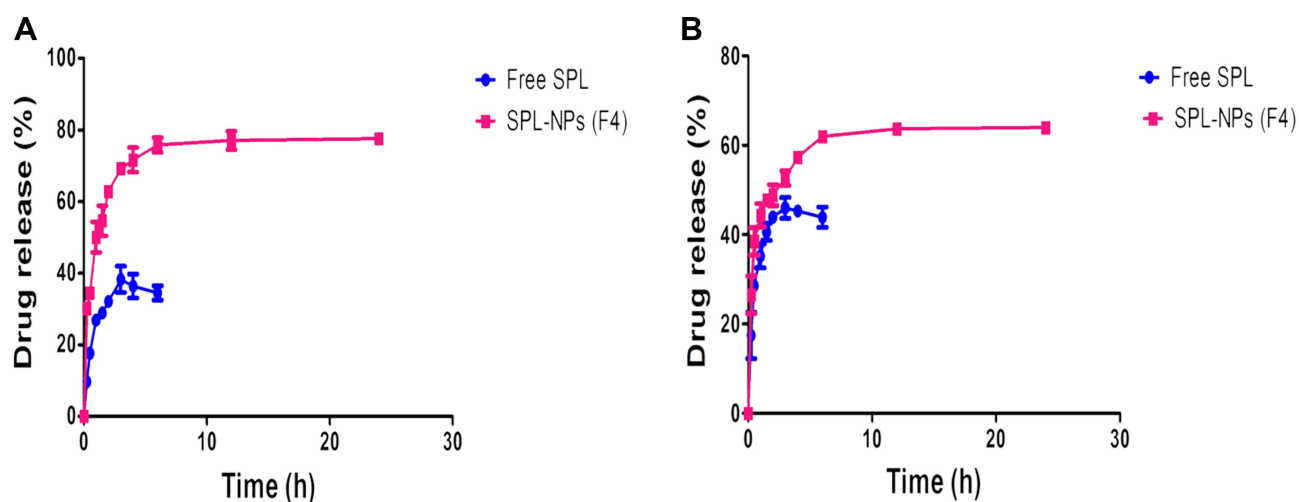

Figure 3 In vitro dissolution results in: (**A**) 0.1N HCl (pH 1.2) and (**B**) 0.066M phosphate buffer (pH 6.8) from the optimized SPL PLGA NPs (F4) compared to the free drug.

Table 2 Kinetic Analysis of Drug Release Data

Dissolution Medium	Correlation Coefficient (r^2)			Release Order	Korsmeyer		Main Transport Mechanism
	Zero Order	First Order	Higuchi Model		r^2	n*	
In 0.1N HCl (pH 1.2)	0.778	0.861	<u>0.937</u>	Higuchi	0.315	0.955	Fickian
In 0.066M phosphate buffer (pH 6.8)	0.779	0.867	<u>0.899</u>	Higuchi	0.243	0.903	Fickian

Note: *n, diffusional exponent.

For the SPL NPs formulation, a biphasic drug release pattern indicated by burst release at early stage could be attributed to the fast dissolution of un-encapsulated drug at the NPs' surface. After the initial burst release phase, relatively slow drug release was found, possibly owing to the aqueous dissolution medium penetration through the hydrophobic polymeric matrix followed by slow diffusion of the drug.[18] PLGA 75:25 has a carboxylic end group with higher hydrophilicity and water absorbing capacity where hydration occurs faster than hydrolysis. Hence, the NP system is eroded via bulk degradation of polymer matrix permitting the drug release.[63] The therapeutic drug concentrations may be provided by the rapid release and could be maintained by the drug release up to 24 h.[64]

Release Kinetics

After the release data analysis of the investigated SPL NPs using different kinetic models, the in vitro dissolution data best fitted the Higuchi diffusion release model with the highest r^2 value compared to the other kinetic models (Table 2). The drug release from both media was described by a Fickian mechanism ($n<0.45$). This model describes the time-dependent release of drug from an insoluble polymer matrix based on Fickian diffusion.[65]

In vivo Assessment of the Antischistosomal Abilities of Drugs Regimens

This experimental study was conducted for 9 weeks on female BALB-c mice infected with *S. mansoni* (Egyptian strain). The treated mice groups were given at the 6th WPI either SPL free drug (as a single dose of 400 mg/kg) or F4 (as a single dose equivalent to 400 mg/kg) or PZQ (as a dose of 500 mg/kg in two successive days). All drugs were administered by oral gavage using a mouse feeding needle, in a volume of 200 µL/mouse in the 6th week post infection (WPI). Control mice groups were either left without treatment or given plain F4 to ensure its therapeutic ineffectiveness on the infection. The antischistosomal effect of these drug regimens was assessed, following euthanasia, by the following parameters:

Liver and Spleen Indices

Mice treatment with SPL free drug, F4, and PZQ caused significant (ρ=0.001, 0.001, and <0.001, respectively) reduction in spleen index (by 37.38%, 39.32%, and 57.28%, respectively) compared to control infected non-treated mice group (Table 3).

Table 3 Liver and Spleen Indices Following Treatment of *Schistosoma mansoni* (Egyptian Strain)-Infected Mice by SPL Free Drug, SPL-Loaded PLGA NPs (F4), and PZQ

Group (n)	Spleen Index			Liver Index		
	Mean ± (SD)	% of Reduction*	ANOVA (ρ value)	Mean± (SD)	% of Reduction*	ANOVA (ρ value)
Infected non-treated control (4)	2.06 (0.13)			9.56 (0.27)		
Control solvent- administrated (4)	1.99 (0.15)			9.61 (0.22)		
SPL free drug (9)	1.29 (0.40)	37.38	0.001	7.62 (1.24)	20.29	0.020
SPL-loaded PLGA NPs (9)	1.25 (0.28)	39.32	0.001	7.43 (0.90)	22.28	0.009
PZQ (4)	0.88 (0.00)	57.28	0.000	7.01 (0.96)	26.67	0.007

Notes: n: Number of euthanized mice, *Percentage of reduction is calculated as regards the infected untreated mice group as: (Mean of a parameter in the control group – mean of the parameter in the treated group) / Mean of parameter in the control group × 100.
Abbreviations: SPL, spironolactone; SPL-loaded PLGA NPs, spironolactone-loaded poly(lactic-co-glycolic acid) nanoparticles; PZQ, praziquantel.

Furthermore, liver index showed significant ($p<0.05$, <0.01, and <0.01, respectively) reduction (by 20.29%, 22.28%, and 26.67%, respectively) on the use of the these drug regimens when compared to the control infected group (Table 3).

The limitation of liver and spleen enlargement and improvement of their condition may be connected to the overall reduction in worm and egg burdens following treatment. Also, that improvement may contribute to spironolactone anti-inflammatory properties.[66] Also, SPL lowers portal hypertension by improvement of liver fibrosis and inhibition of intrahepatic vasoconstriction,[67] thus improving the liver and spleen enlargement that occurs as a result of portal hypertension produced by *Schistosoma* egg granuloma formation.[68]

These results are in agreement with Guerra et al,[4] who found that the pathology normally associated with the deposition of *Schistosoma* eggs in the spleen and liver was clearly ameliorated by administration of SPL for 5 days as 100 mg/kg in the 6th WPI ($p<0.05$ to $p<0.001$). They attributed that effect to reduction in the worm burden and oviposition reduction following treatment, as well as to the pharmacological properties of SPL to treat edematous conditions.[69] It is worth mentioning that the SPL effect on spleen and liver indices is potentiated by using the nanoparticle form of the drug, as the reduction reaches 39.32% and 22.28%, respectively. The drug entrapment in a nanoparticulate system could pave the way for improved stability when in contact with biological fluids, as well as high drug-loading capacities, cellular uptake or drug targeting to certain tissues, and offering controlled drug release effects.[70]

Total and Female Worm Burdens

Perfusion of the portosystemic veins in mice revealed *Schistosoma* worms that were washed, counted, and sexually differentiated. All given therapeutic protocols (SPL alone, F4, and PZQ) significantly ($p<0.005$, <0.001, <0.005, respectively) reduced the total worm count (by 46.15%, 61.54%, and 61.54%, respectively), compared with control infected mice group (Table 4).

Interestingly, the mean count of revealed female worms in mice treated with F4 and in mice treated with PZQ were reduced significantly ($p<0.05$ for both) (by 66.67%) when compared to control infected group. Meanwhile, SPL free drug treatment reduced the revealed female worm count by 33.33% which was not significantly different from the control mice (Table 4).

It was clear that the reduction rates were higher with the nanoparticle form of the drugs, reaching levels similar to PZQ (the drug of choice), as both are superior to the drug free form in that parasitological parameter.

This effect was also documented by Guerra et al[4] as oral treatment with a single dose of SPL achieved total and female worm burden reductions by 73.8% ($p<0.001$) and 69.7% ($p<0.001$), respectively. Our results are somewhat lower than those of Guerra et al,[4] probably owing to different experiment circumstances such as *Schistosom*a strain, mice module, and infecting dose. These effects were mostly related to the SPL effect on worm tegument and suckers and motor activity of these worms as stated by the in vitro studies of Aminou and Abdel Rahman.[22]

Hepatic and Intestinal Egg Loads

We found a reduction in female worm count, accompanied with reduction in fecundity which was evidenced by the significant reduction in hepatic and intestinal egg loads observed following treatment with different used drug regimens

Table 4 Worm Burden Following Treatment of *Schistosoma mansoni* (Egyptian Strain)-Infected Mice by SPL Free Drug, SPL-Loaded PLGA NPs (F4), and PZQ

Group (n)	Male Worm Mean ± (SD)	Female Worm Mean ± (SD)	% of Reduction*	ANOVA (p value)	Total Worm Mean ± (SD)	% of Reduction*	ANOVA (p value)
Infected Control (4)	7 (1)	6 (1)			13 (0)		
Control Solvent (4)	6 (1)	6 (1)			12 (1)		
SPL Free Drug (9)	3 (1)	4 (2)	33.33		7 (3)	46.15	0.003
SPL-loaded PLGA NPs (9)	3 (2)	2 (2)	66.67	0.016	5 (3)	61.54	0.000
PZQ (4)	4 (1)	2 (1)	66.67	0.011	5 (1)	61.54	0.002

Notes: n: Number of euthanized mice, *Percentage of reduction is calculated as regards the infected untreated mice group as: (Mean of a parameter in the control group – mean of the parameter in the treated group) / Mean of parameter in the control group.
Abbreviations: SPL, spironolactone; SPL-loaded PLGA NPs, spironolactone-loaded poly(lactic-co-glycolic acid) nanoparticles; PZQ, praziquantel.

Table 5 Tissue Egg Load Following Treatment by SPL Free Drug, SPL-Loaded PLGA NPs (F4), and PZQ of *Schistosoma mansoni* (Egyptian Strain)-Infected Mice

Group (n)	Hepatic Egg Load MEAN ± (SD)	% Reduction*	ANOVA (ρ value)	Intestinal Egg Load Mean ± (SD)	% Reduction*	ANOVA (ρ value)
Infected Control (4)	26.58 (3.79)			16.8 (0.0)		
Control Solvent (4)	20.67 (2.75)			15.0 (0.7)		
SPL Free Drug (9)	14.79 (4.84)	44.36	0.000	8.6 (3.5)	48.81	0.004
SPL-loaded PLGA NPS (9)	11.23 (3.84)	57.75	0.000	7.7 (4.6)	54.17	0.001
PZQ (4)	8.44 (0.55)	68.25	0.000	6.0 (0.8)	64.29	0.001

Notes: *n*: Number of euthanized mice, *Percentage of reduction is calculated as regards the infected untreated mice group as: (Mean of a parameter in the control group – mean of the parameter in the treated group) / Mean of parameter in the control group.
Abbreviations: SPL, spironolactone; SPL-loaded PLGA NPs, spironolactone-loaded poly(lactic-co-glycolic acid) nanoparticles; PZQ, praziquantel.

(Table 5). We found that all assessed treatment regimens (SPL free drug, F4, and PZQ) induced statistically significant reductions ($\rho < 0.001$) in the calculated hepatic egg load (by 44.36%, 57.75%, and 68.25%, respectively). Moreover, these regimens induced statistically significant ($\rho < 0.005$, ≤ 0.001, and ≤ 0.01, respectively) reduction in small intestinal egg burden (by 48.81%, 54.17%, 64.29%, respectively) on comparing with control infected non-treated mice group (Table 5).

From the previous results, it was also obvious that the nanoparticle form of the drug (F4) is superior to the free form as regards liver and intestinal tissue egg load (57.75% and 54.17%, respectively). This is matching with our finding of marked effect on female worms of the nanoparticle preparation. However, this effect is still lower than PZQ reduction rates (68.25% and 64.29%, respectively).

The egg burden reduction is a cause of worm reduction and a reason for liver and spleen improvement. A significant reduction in eggs collected from the intestine or feces has been described with other antischistosomal compounds as a result of their effect on female worms.[71,72]

Oogram Studies

As illustrated in Table 6, all tested drug regimens showed significant decrease ($\rho < 0.001$) in immature ovum ratios accompanied with significant increase in the dead egg ratios ($\rho < 0.001$) when compared to the control untreated group (50% immature eggs and 21% dead eggs). These regimens caused a shift of the oogram pattern, reducing immature eggs (to reach 27%, 28%, and 21%, respectively) and increasing the dead eggs (to reach 49%, 50%, and 59%, respectively).

Also, from these results, the F4 effect was superior to free drug in reducing immature egg (28% and 27%, respectively) and in increasing the dead egg (50% and 49%, respectively). That shift of oogram curve pattern is evidence for reduced oviposition and increased healing processes.

Table 6 Oogram Patterns Following Treatment of *Schistosoma mansoni* (Egyptian Strain)-Infected Mice by SPL Free Drug, SPL-Loaded PLGA NPs, and PZQ

Group (n)	Immature Egg% Mean ± (SD)	ANOVA (ρ value)	Mature Egg% Mean ± (SD)	Dead Egg % Mean ± (SD)	ANOVA (ρ value)
Infected Control (4)	50 (4)		29 (2)	21 (3)	
Solvent Control (4)	56 (8)		28 (11)	17 (4)	
SPL Free Drug (9)	27 (5)	0.000	24 (5)	49 (6)	0.000
SPL-loaded PLGA NPs (9)	28 (6)	0.000	22 (7)	50 (5)	0.000
PZQ (4)	21 (2)	0.000	20 (6)	59 (9)	0.000

Abbreviations: SPL, spironolactone; SPL-loaded PLGA NPs, spironolactone-loaded poly(lactic-co-glycolic acid) nanoparticles; PZQ, praziquantel.

Oogram changes were also documented by Guerra et al[4] as the single dose of SPL produced a reduction of 73.4% ($\rho \leq 0.001$) in the number of immature eggs, while the 5-day administration of the drug achieved immature egg reduction of 75.6% ($\rho \leq 0.001$) in a dose-dependent manner.

Electron Microscope Studies

The worms recovered from portosystemic vein perfusion were processed, fixed in glutaraldehyde, and examined by the high power of the scanning electron microscope to document the effect of tested drugs regimen on the integrity of tegument and outer lining of worms.

The worms subjected to in vivo treatment by SPL showed erosion, fissuring, and deformities, especially at the anterior region near suckers (Figure 4A and B). Moreover, the tubercles on male tegument were disrupted, lost arrangement with loss of some spines (Figure 4A and D). The female worms were severely affected with fissures, holes, and exposure of subtegumental tissue (Figure 4B and C).

The electron microscope studies explored the dominance of nanoparticles over the free drugs on mediating their antischistosomal effects. The adult male worms treated in vivo with F4 formula showed more severe erosions, fissuring, and lost integrity, especially on suckers (the attachment organ of the worm that protects it from being swept with the blood stream) (Figure 5A and D). Also, the effect on the female worms was exaggerated with marked erosions, peeling, fissuring, lost folds arrangement, and exposure of subtegumental tissue (Figure 5B and C).

All of these findings explain the drug effect on the neuromuscular activity of the worm and explain the reduction seen in worm and female worm burden and in turn fecundity and egg burden. This agrees with Adler[73] who stated that
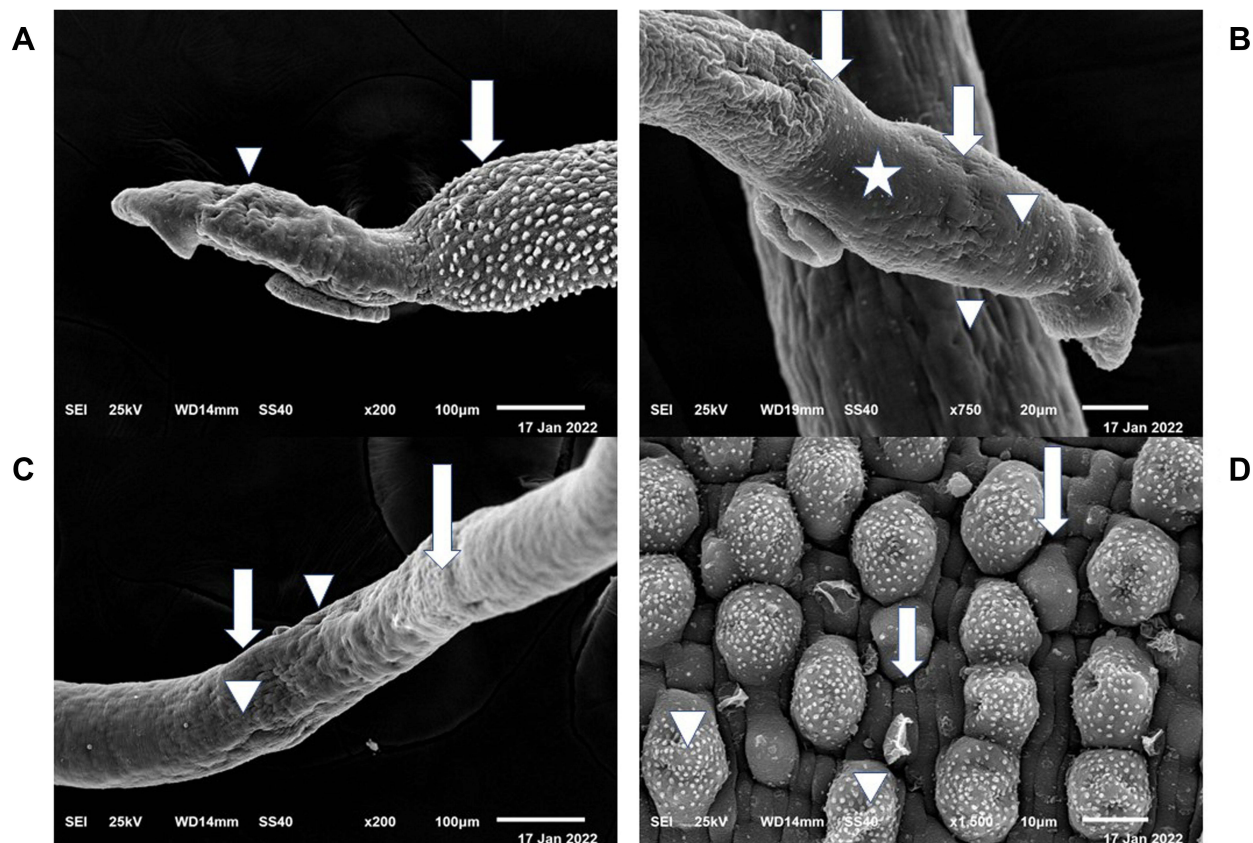

Figure 4 Scanning electron microscopic imaging of *Schistosoma* adult worms revealed from mice treated with spironolactone (free drug) as a single dose of 400 mg/kg of mice weight. (**A**) The dorsal surface of male worm showed erosions and fissuring of the tegument especially in the region of suckers (arrowhead). Besides, loosing of tubercles arrangement and integrity were also seen (arrow). (**B**) The dorsal surface of the female worm also showed extensive erosions and fissures (star) making holes with exposing of subtegumental tissue (arrow), and also peeling of tegument and disruption of folds integrity was seen (arrowhead). (**C**) The middle part of female worm showed extensive fissuring and swelling of tegument (arrow) exposing the subtegumental tissue and making holes all over the surface (arrowheads). (**D**) The tubercles on the male worm showed distortion, lost arrangement (arrows), interrupted spines, and peeling (arrowheads).
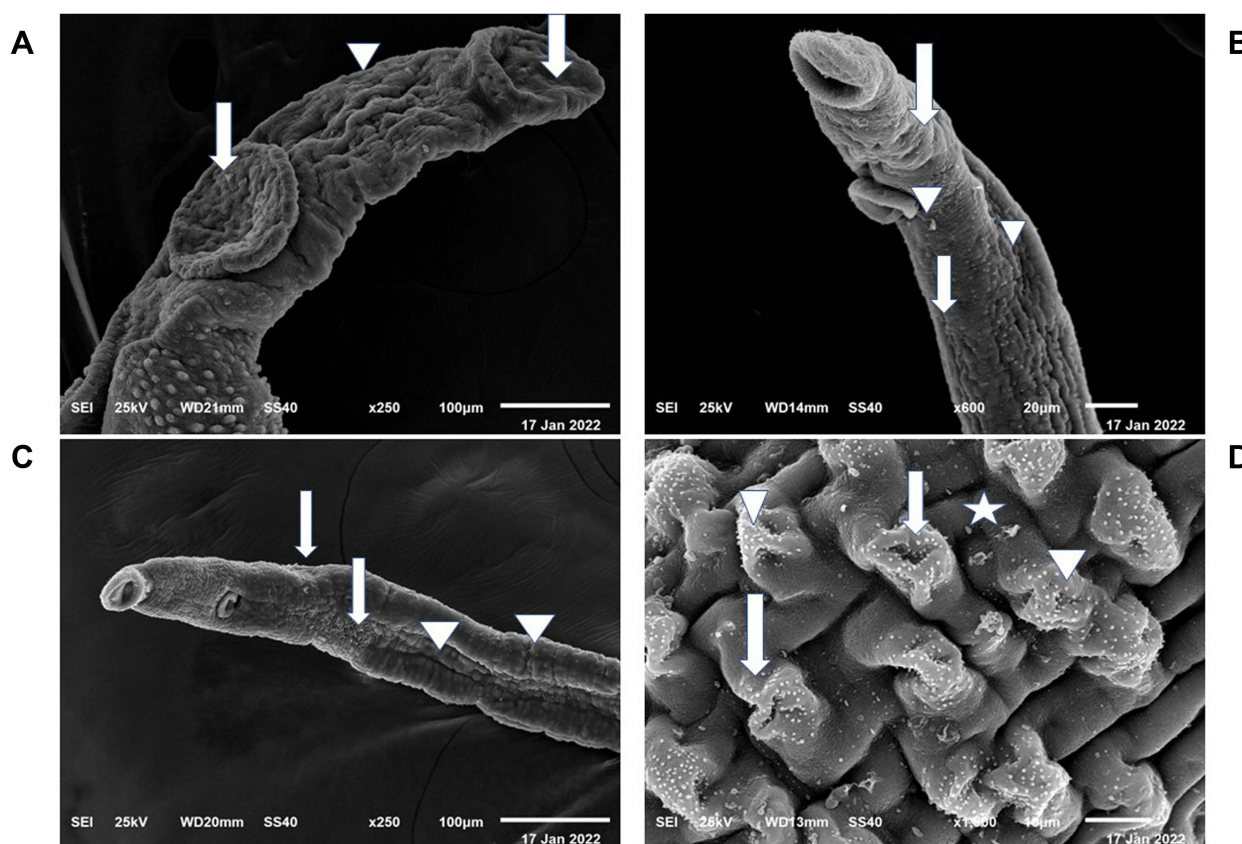
Figure 5 Scanning electron microscopic imaging of *Schistosoma* adult worms revealed from mice treated with SPL PLGA NPs (F4) as a single dose of 400 mg/kg of mice weight. (**A**) The dorsal surface of male worm showed extensive erosions, wrinkling, and fissuring of the tegument especially in the region of suckers (arrowhead). Besides, interrupted integrity and musculature of suckers was obviously seen (arrow). (**B**) The dorsal surface of the female worm especially near suckers showed extensive erosions and fissures making holes with exposing of subtegumental tissue (arrow), and also peeling of tegument and disruption of folds integrity was seen (arrowhead). (**C**) The female worm whole body showed erosion, fissuring (arrows), blebbing, distortion, lost folding, and subtegumental tissue exposure (arrowheads) which affect suckers' integrity and motor activity. (**D**) The tubercles on the male worm surface showed extensive disruption (arrows) and lost and distorted spines (arrowheads) with some eruptions on surface (star).

Schistosoma tegument is an important target for drugs. These findings were also analogous with the reports of Guerra et al[4] and Aminou and Abdel Rahman,[22] who tested the effect of in vitro incubation of SPL on *Schistosoma* worms.

The exact mechanism for SPL antischistosomal features is still not clear. It could be linked to its inhibition of androgen production (prototypic mineralocorticoid receptor antagonist), as the adrenal hormones affect the survival and oviposition of schistosomes both in vitro and in vivo by inhibiting glucose metabolism.[74,75] But the most accepted explanation is the effect of drug on the neuromuscular system of *S. mansoni* that leads to decreased motility, induced contraction, and subsequent tegument erosions and sloughing as evidenced by the in vitro studies on adult worms to confirm a concentration dependent effect on the neuromuscular system of the parasite.

To the best of our knowledge, this is the first in vivo study exploring the effect of spironolactone nanoparticle (F4) on murine *schistosomiasis*. It is worth mentioning that all the observed tegumental changes were more exaggerated in worms following F4 treatment than the free form of the drug. This could be the most proper explanation for the higher reduction rates of parasitological parameters and improvement of the general condition in that mice group than the one received the free drug.

Our study uses SPL-loaded PLGA NPs which showed better results than free drug. Our results were in agreement with AboSheishaa[76] whose study used PLGA NPs loaded with PZQ. The authors found that PLGA NPs improved the antischistosomal effects of PZQ with highly significant reduction in mean total worm burden, the highest elevation of the percentage of dead ova (95.31%), with complete disappearance of immature ova and the highest reduction of egg load in hepatic tissue by 97.1%.[76] Another team work[77] potentiate the antischistosomal abilities of the synthetic preparation (the

−6,60-dinitrohinokinin (DNHK)) by incorporation to PLGA nanoparticles. The in vitro incubation of adult worms was associated with marked reduction in motor activity and egg production. Luz et al, 2012,[78] incorporated curcumin into PLGA nanoparticles and tested its ability in vitro on *Schistosoma* worms. They declared that curcumin-loaded PLGA nanoparticles caused partial alterations in the tegument of the adult worms in concentrations nearly 40 μM, revealed by the presence of vesicles in its structure, while that action was produced by the curcumin free drug only after 100 μM. Also, other parameters (such as the separation of male and female worms) were seen earlier with the drug-loaded NPs than the free drug.

Histopathological Study

Schistosoma mansoni induce inflammation in the liver tissue with interstitial inflammatory cellular infiltrate, sometimes with some necrotic hepatocytes.[79] Moreover, a granulomatous reaction around a central living bilharzial ova surrounded by multiple inflammatory cells and fibrosis is the main characteristic feature of infection (Figure 6A and B).

Treatment of infected mice with SPL and F4 ameliorated the liver pathology as evidenced by the decrease of infiltrated inflammatory cells and granuloma numbers (Figure 6C and E). The eggs are partially degenerated and surrounding granulomas are smaller, healed, and fibrosed (Figure 6D and F). This improvement is thought to be a result of the drug-induced reduction in female worms count and reduction in oviposition and also of the drug anti-inflammatory effect.[66] Additionally, the amendment of liver pathology induced by F4 could be elucidated by the smart targeting of the discontinued epithelium around the lodged eggs. PLGA nanoparticles are considered an excellent drug carrier with high targeted drug delivery ability.[80] Hence, it can move through the interstitial spaces of discontinued
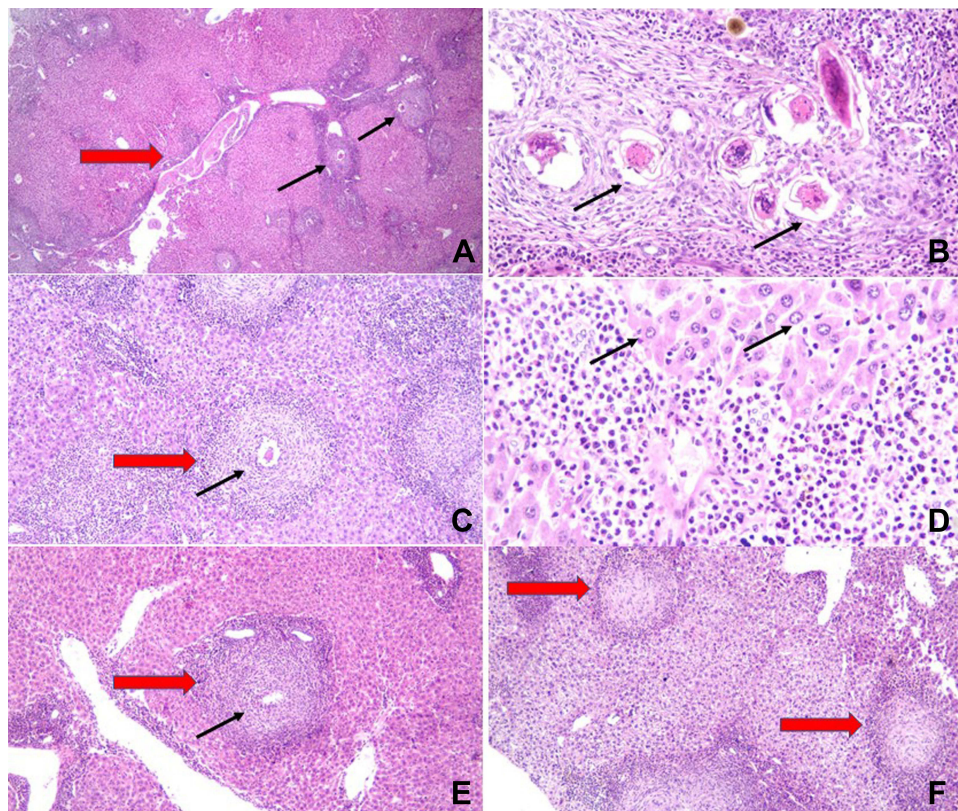

Figure 6 Histopathological studies of liver sections from mice infected with *Schistosoma mansoni*: (**A** and **B**) Liver sections from infected untreated control mice: (**A**) showing a worm in portal vein (red arrow) with associated multiple epithelioid granulomas surrounding viable eggs (black arrows) (H+E; magnification ×40). (**B**) Higher magnification in liver sections of the control mice showing the epithelioid granuloma with viable eggs within (arrow) (H+E; magnification ×200). (**C** and **D**) Liver sections from infected mice treated with SPL (free drug) as 400 mg/kg: (**C**) showing evident decrease in the number of epithelioid granulomas having an ovum in the center of few of them (black arrow) (H=E; magnification ×100). (**D**) gradual replacement of epithelioid granulomas with mixed chronic inflammatory cells (H+E; magnification ×400). (**E** and **F**) Liver section from infected mice treated with SPL PLGA NPs (F4) as 400 mg/kg: (**E**) showing marked reduction in the number of epithelioid granulomas with no detected viable ova (black arrow) (H+E; magnification ×100). (**F**) showing multiple healed epithelioid granulomas devoid of any viable eggs (H+E; magnification ×100).

epithelial cells, accumulating more SPL around the eggs. The prepared nanoparticles could provide a distinct niche for themselves by acting as a carrier-driven cellular entry mechanism independent of the solubility or permeability of the entrapped drug. The unique properties of these carrier systems could be used for SPL (class II drug with low solubility, high permeability).[70] This in turn causes in situ lessening of the eggs' ability to induce granulomata. Mokbel et al, 2020,[81] reported similar histopathological effects when testing the antischistosomal activity of curcumin-loaded nanoparticles, especially when combined with PZQ.

Conclusion

In conclusion, repurposing SPL-loaded PLGA NPs in a single oral dose of 400 mg/kg as a new potential antischistosomal drug paved the way to be used as an alternative to the PZQ drug. We successfully applied the emulsion solvent evaporation technique to incorporate SPL into PLGA nanoparticles with high efficiency. SPL-loaded NPs caused extensive damage to adult worms on tegument and suckers, leading to the death of the parasites in less time, plus marked improvement in liver pathology. Further studies aim to investigate the protective effect of SPL-loaded PLGA NPs in the schistosomiasis animal model in progress by our group. In the future, the in-vivo efficacy of the SPL-loaded NPs is required to confirm our findings.

Acknowledgment

Disclosure

The authors declare no conflicts of interest in this work.

References

1. Porto R, Mengarda AC, Cajas RA, et al. Antiparasitic properties of cardiovascular agents against human intravascular parasite Schistosoma mansoni. *Pharmaceuticals*. 2021;14(7):686. doi:10.3390/ph14070686
2. Aula OP, McManus DP, Jones MK, Gordon CA. Schistosomiasis with a Focus on Africa. *Trop Med Int Health*. 2021;6(3):109. doi:10.3390/tropicalmed6030109
3. World Health Organization. Schistosomiasis; 2022. Available from: https://www.who.int/news-room/fact-sheets/detail/schistosomiasis. Accessed February 8, 2023.
4. Guerra RA, Silva MP, Silva TC, et al. In vitro and in vivo studies of spironolactone as an antischistosomal drug capable of clinical repurposing. *Antimicrob Agents Chemother*. 2019;63(3):e01722–e01718. doi:10.1128/AAC.01722-18
5. von Seidlein L, Dondorp A. Fighting fire with fire: mass antimalarial drug administrations in an era of antimalarial resistance. *Expert Rev Anti Infect Ther*. 2015;13(6):715–730. doi:10.1586/14787210.2015.1031744
6. Radwan A, El-Lakkany NM, William S, et al. A novel praziquantel solid lipid nanoparticle formulation shows enhanced bioavailability and antischistosomal efficacy against murine S. mansoni infection. *Parasit Vectors*. 2019;12(1):304. doi:10.1186/s13071-019-3563-z
7. Amara RO, Ramadan AA, El-Moslemany RM, Eissa MM, El-Azzouni MZ, El-Khordagui LK. Praziquantel–lipid nanocapsules: an oral nanotherapeutic with potential Schistosoma mansoni tegumental targeting. *Int J Nanomed*. 2018;13:4493. doi:10.2147/IJN.S167285
8. Roquini DB, Cogo RM, Mengarda AC, et al. Promethazine exhibits antiparasitic properties in vitro and reduces worm burden, egg production, hepatomegaly, and splenomegaly in a schistosomiasis animal model. *Antimicrob Agents Chemother*. 2019;63(12):e01208–e01219. doi:10.1128/AAC.01208-19
9. Patra JK, Das G, Fraceto LF, et al. Nano based drug delivery systems: recent developments and future prospects. *J Nanobiotechnology*. 2018;16(1):71.
10. Haggag YA, Abosalha AK, Tambuwala MM, et al. Polymeric nanoencapsulation of zaleplon into PLGA nanoparticles for enhanced pharmacokinetics and pharmacological activity. *Biopharm Drug Dispos*. 2021;42(1):12–23. doi:10.1002/bdd.2255
11. Silva TC, Mengarda AC, Silva BC, et al. New evidence for tamoxifen as an antischistosomal agent: in vitro, in vivo and target fishing studies. *Future Med Chem*. 2021;13(11):945–957. doi:10.4155/fmc-2020-0311
12. de Brito MG, Mengarda AC, Oliveira GL, et al. Therapeutic effect of diminazene aceturate on parasitic blood fluke Schistosoma mansoni infection. *Antimicrob Agents Chemother*. 2020;64(11):e01372–e01320. doi:10.1128/AAC.01372-20
13. Lago EM, Silva MP, Queiroz TG, et al. Phenotypic screening of nonsteroidal anti-inflammatory drugs identified mefenamic acid as a drug for the treatment of schistosomiasis. *EBioMedicine*. 2019;43:370–379. doi:10.1016/j.ebiom.2019.04.029
14. Barbosa EJ, Löbenberg R, de Araujo GLB, Bou-Chacra NA. Niclosamide repositioning for treating cancer: challenges and nano-based drug delivery opportunities. *Eur J Pharm Biopharm*. 2019;141:58–69. doi:10.1016/j.ejpb.2019.05.004
15. He C, Duan L, Zheng H, Song L, Huang M. An explainable framework for drug repositioning from disease information network. *Neurocomputing*. 2022;511:247–258. doi:10.1016/j.neucom.2022.09.063
16. Haggag YA, Yasser M, Tambuwala MM, El Tokhy SS, Isreb M, Donia AA. Repurposing of Guanabenz acetate by encapsulation into long-circulating nanopolymersomes for treatment of triple-negative breast cancer. *Int J Pharm*. 2021;600:120532. doi:10.1016/j.ijpharm.2021.120532

17. Manolis AA, Manolis TA, Melita H, Manolis AS. Spotlight on spironolactone oral suspension for the treatment of heart failure: focus on patient selection and perspectives. *Vasc Health Risk Manag*. 2019;15:571. doi:10.2147/VHRM.S210150

18. Shamma RN, Aburahma MH. Follicular delivery of spironolactone via nanostructured lipid carriers for management of alopecia. *Int J Nanomed*. 2014;9:5449. doi:10.2147/IJN.S73010

19. Lainscak M, Pelliccia F, Rosano G, et al. Safety profile of mineralocorticoid receptor antagonists: spironolactone and eplerenone. *Int J Cardiol*. 2015;200:25–29. doi:10.1016/j.ijcard.2015.05.127

20. Papademetriou V, Toumpourleka M, Imprialos KP, Alataki S, Manafis A, Stavropoulos K. The role of mineralocorticoid receptor antagonists in heart failure with reduced ejection fraction. *Curr Pharm Des*. 2018;24(46):5517–5524. doi:10.2174/1381612825666190219141326

21. Manolis AA, Manolis TA, Melita H, Manolis AS. Eplerenone versus spironolactone in resistant hypertension: an efficacy and/or cost or just a men's issue? *Curr Hypertens Rep*. 2019;21(3):1–14. doi:10.1007/s11906-019-0924-0

22. Aminou H, Abdel Rahman A. Spironolactone: a promising anti-schistosomal drug as revealed by scanning electron microscopy of adult worms. *Parasitol United J*. 2020;13(2):121–125. doi:10.21608/puj.2020.33168.1076

23. Pandita D, Kumar S, Lather V. Hybrid poly (lactic-co-glycolic acid) nanoparticles: design and delivery prospectives. *Drug Discov Today*. 2015;20 (1):95–104. doi:10.1016/j.drudis.2014.09.018

24. Danhier F, Ansorena E, Silva JM, Coco R, Le breton A, Préat V. PLGA-based nanoparticles: an overview of biomedical applications. *J Control Release*. 2012;161(2):505–522. doi:10.1016/j.jconrel.2012.01.043

25. Liang Q, Xiang H, Li X, et al. Development of rifapentine-loaded PLGA-based nanoparticles: in vitro characterisation and in vivo study in mice. *Int J Nanomed*. 2020;15:7491. doi:10.2147/IJN.S257758

26. Lai P, Daear W, Löbenberg R, Prenner EJ. Overview of the preparation of organic polymeric nanoparticles for drug delivery based on gelatine, chitosan, poly (d, l-lactide-co-glycolic acid) and polyalkylcyanoacrylate. *Colloids Surfaces B*. 2014;118:154–163. doi:10.1016/j.colsurfb.2014.03.017

27. Alshamsan A. Nanoprecipitation is more efficient than emulsion solvent evaporation method to encapsulate cucurbitacin I in PLGA nanoparticles. *Saudi Pharm J*. 2014;22(3):219–222. doi:10.1016/j.jsps.2013.12.002

28. Lassalle V, Ferreira ML. PLA nano-and microparticles for drug delivery: an overview of the methods of preparation. *Macromol Biosci*. 2007;7 (6):767–783. doi:10.1002/mabi.200700022

29. Fessi H, Puisieux F, Devissaguet JP, Ammoury N, Benita S. Nanocapsule formation by interfacial polymer deposition following solvent displacement. *Int J Pharm*. 1989;55(1):R1–R4. doi:10.1016/0378-5173(89)90281-0

30. Abd El Hady WE, Mohamed EA, Soliman O-AE-A, El-Sabbagh HM. In vitro–in vivo evaluation of chitosan-PLGA nanoparticles for potentiated gastric retention and anti-ulcer activity of diosmin. *Int J Nanomed*. 2019;14:7191. doi:10.2147/IJN.S213836

31. Gupta H, Aqil M, Khar RK, Ali A, Bhatnagar A, Mittal G. Sparfloxacin-loaded PLGA nanoparticles for sustained ocular drug delivery. *Nanomedicine*. 2010;6(2):324–333. doi:10.1016/j.nano.2009.10.004

32. Jangid AK, Solanki R, Patel S, Pooja D, Kulhari H. Genistein encapsulated inulin-stearic acid bioconjugate nanoparticles: formulation development, characterization and anticancer activity. *Int J Biol Macromol*. 2022;206:213–221. doi:10.1016/j.ijbiomac.2022.02.031

33. Puri V, Chaudhary KR, Singh A, Singh C. Inhalation potential of N-Acetylcysteine loaded PLGA nanoparticles for the management of tuberculosis: in vitro lung deposition and efficacy studies. *Curr Res Pharmacol Drug Dis*. 2022;100084. doi:10.1016/j.crphar.2022.100084

34. Li Y, Li M, Rantanen J, Yang M, Bohr A. Transformation of nanoparticles into compacts: a study on PLGA and celecoxib nanoparticles. *Int J Pharm*. 2022;611:121278. doi:10.1016/j.ijpharm.2021.121278

35. Mehdizadeh M, Rouhani H, Sepehri N, et al. Biotin decorated PLGA nanoparticles containing SN-38 designed for cancer therapy. *Artif Cells, Nanomed Biotechnol*. 2017;45(3):495–504. doi:10.1080/21691401.2016.1178130

36. Martin AN, Swarbrick J, Cammarata A. Physical pharmacy: physical chemical principles in the pharmaceutical sciences; 1993.

37. Higuchi T. Mechanism of sustained-action medication. Theoretical analysis of rate of release of solid drugs dispersed in solid matrices. *J Pharm Sci*. 1963;52(12):1145–1149. doi:10.1002/jps.2600521210

38. Ritger PL, Peppas NA. A simple equation for description of solute release I. Fickian and non-fickian release from non-swellable devices in the form of slabs, spheres, cylinders or discs. *J Control Release*. 1987;5(1):23–36. doi:10.1016/0168-3659(87)90034-4

39. Smithers SR, Terry RJ. The infection of laboratory hosts with cercariae of Schistosoma mansoni and the recovery of the adult worms. *Parasitology*. 1965;55(4):695–700. doi:10.1017/s0031182000086248

40. Cheever AW. Conditions affecting the accuracy of potassium hydroxide digestion techniques for counting Schistosoma mansoni eggs in tissues. *Bull World Health Organ*. 1968;39(2):328–331.

41. Pellegrino J, Oliveira CA, Faria J, Cunha AS. New approach to the screening of drugs in experimental schistosomiasis mansoni in mice. *Am J Trop Med Hyg*. 1962;11:201–215. doi:10.4269/ajtmh.1962.11.201

42. Ibrahim EI, Abou-El-Naga IF, El-Temsahy MM, Elsawy ESA, Makled S, Mogahed NMFH. A single oral dose of celecoxib-loaded solid lipid nanoparticles for treatment of different developmental stages of experimental schistosomiasis mansoni. *Acta Trop*. 2022;229:106342. doi:10.1016/j.actatropica.2022.106342

43. Ozakar E, Cetin M, Ates O, Hacimuftuoglu A. Nifedipine-loaded polymeric nanoparticles: preparation and in vitro characterization. *Pak J Pharm Sci*. 2019;32(2):547–554.

44. Kalimouttou S, Lahiani-Skiba M, Naouli N, Lin VS, Skiba M. Evaluation of the paromomycin loading characteristics in nanoprecipitated PLGA nanospheres. *NSTI Nanotech Tech Proceed*. 2008;2:407–410.

45. Nagavarma B, Yadav HK, Ayaz A, Vasudha L, Shivakumar H. Different techniques for preparation of polymeric nanoparticles-a review. *Asian J Pharm Clin Res*. 2012;5(3):16–23.

46. Budhian A, Siegel SJ, Winey KI. Haloperidol-loaded PLGA nanoparticles: systematic study of particle size and drug content. *Int J Pharm*. 2007;336(2):367–375. doi:10.1016/j.ijpharm.2006.11.061

47. Om H, El-Naggar ME, El-Banna M, et al. Combating atherosclerosis with targeted Diosmin nanoparticles-treated experimental diabetes. *Invest New Drugs*. 2020;38(5):1303–1315. doi:10.1007/s10637-020-00905-6

48. Calderó G, Rodríguez-Abreu C, González A, Monge M, García-Celma MJ, Solans C. Biomedical perfluorohexane-loaded nanocapsules prepared by low-energy emulsification and selective solvent diffusion. *Mater Sci Eng*. 2020;111:110838. doi:10.1016/j.msec.2020.110838

49. Youshia J, Ali ME, Lamprecht A. Artificial neural network based particle size prediction of polymeric nanoparticles. *Eur J Pharm Biopharm*. 2017;119:333–342. doi:10.1016/j.ejpb.2017.06.030

50. Mainardes RM, Evangelista RC. PLGA nanoparticles containing praziquantel: effect of formulation variables on size distribution. *Int J Pharm*. 2005;290(1–2):137–144. doi:10.1016/j.ijpharm.2004.11.027

51. Lamprecht A, Ubrich N, Yamamoto H, et al. Design of rolipram-loaded nanoparticles: comparison of two preparation methods. *Journal Controlled Res*. 2001;71(3):297–306. doi:10.1016/S0168-3659(01)00230-9

52. Alkholief M, Kalam MA, Anwer MK, Alshamsan A. Effect of solvents, stabilizers and the concentration of stabilizers on the physical properties of Poly (d, l-lactide-co-glycolide) nanoparticles: encapsulation, in vitro release of indomethacin and cytotoxicity against HepG2-cell. *Pharmaceutics*. 2022;14(4):870. doi:10.3390/pharmaceutics14040870

53. Hernández-Giottonini KY, Rodríguez-Córdova RJ, Gutiérrez-Valenzuela CA, et al. PLGA nanoparticle preparations by emulsification and nanoprecipitation techniques: effects of formulation parameters. *RSC Adv*. 2020;10(8):4218–4231. doi:10.1039/C9RA10857B

54. Müller RH, Jacobs C. Buparvaquone mucoadhesive nanosuspension: preparation, optimisation and long-term stability. *Int J Pharm*. 2002;237(1–2):151–161. doi:10.1016/S0378-5173(02)00040-6

55. Seko I, Tonbul H, Tavukçuoğlu E, et al. Development of curcumin and docetaxel co-loaded actively targeted PLGA nanoparticles to overcome blood brain barrier. *J Drug Deliv Sci Technol*. 2021;66:102867. doi:10.1016/j.jddst.2021.102867

56. Bayas JP, Sumithra M. QbD method to the formulation and development of a spironolactone immediate-release tablet with enhanced dissolving research. *Materials Today*. 2022;2022:95.

57. Guerini M, Perugini P, Grisoli P. Evaluation of the Effectiveness of N-Acetylcysteine (NAC) and N-acetylcysteine-cyclodextrins multi-composite in Pseudomonas aeruginosa biofilm formation. *Appli Sci*. 2020;10(10):3466. doi:10.3390/app10103466

58. Suri R, Neupane YR, Mehra N, et al. Sirolimus loaded chitosan functionalized poly (lactic-co-glycolic acid)(PLGA) nanoparticles for potential treatment of age-related macular degeneration. *Int J Biol Macromol*. 2021;191:548–559. doi:10.1016/j.ijbiomac.2021.09.069

59. Resende R, Viana OMMS, Freitas JTJ, Bonfilio R, Ruela ALM, Araújo M. Analysis of spironolactone polymorphs in active pharmaceutical ingredients and their effect on tablet dissolution profiles. *Braz J Pharm Sci*. 2016;52:613–621. doi:10.1590/s1984-82502016000400005

60. Elkordy AA, Tan XN, Essa EA. Spironolactone release from liquisolid formulations prepared with Capryol™ 90, Solutol® HS-15 and Kollicoat® SR 30 D as non-volatile liquid vehicles. *Eur J Pharm Biopharm*. 2013;83(2):203–223. doi:10.1016/j.ejpb.2012.08.004

61. Kelidari H, Saeedi M, Akbari J, et al. Development and optimisation of spironolactone nanoparticles for enhanced dissolution rates and stability. *AAPS Pharm Sci Tech*. 2017;18(5):1469–1474. doi:10.1208/s12249-016-0621-0

62. Kelidari H, Saeedi M, Akbari J, et al. Formulation optimization and in vitro skin penetration of spironolactone loaded solid lipid nanoparticles. *Colloids Surfaces B*. 2015;128:473–479. doi:10.1016/j.colsurfb.2015.02.046

63. Samadi N, Abbadessa A, Di Stefano A, et al. The effect of lauryl capping group on protein release and degradation of poly (d, l-lactic-co-glycolic acid) particles. *Journal Controlled Res*. 2013;172(2):436–443. doi:10.1016/j.jconrel.2013.05.034

64. Mahmoodi M, Khosroshahi ME, Atyabi F. Laser thrombolysis and in vitro study of tPA release encapsulated by chitosan coated PLGA nanoparticles for AMI. *Int J Biol Biomed Eng*. 2010;4(2):35–42.

65. Ghasemian E, Vatanara A, Rouholamini Najafabadi A, Rouini MR, Gilani K, Darabi M. Preparation, characterization and optimization of sildenafil citrate loaded PLGA nanoparticles by statistical factorial design. *DARU J Pharm Sci*. 2013;21(1):1–10. doi:10.1186/2008-2231-21-68

66. K SASGBKkmdHPR. Spironolactone inhibits production of proinflammatory cytokines, including tumour necrosis factor-α and interferon-γ, and has potential in the treatment of arthritis. *Clin Exp Immunol*. 2003;134(1):151–158. doi:10.1046/j.1365-2249.2003.02249.x

67. Luo W, Meng Y, Ji HL, et al. Spironolactone lowers portal hypertension by inhibiting liver fibrosis, ROCK-2 activity and activating NO/PKG pathway in the bile-duct-ligated rat. *PLoS One*. 2012;7(3):e34230. doi:10.1371/journal.pone.0034230

68. Elbaz T, Esmat G. Hepatic and intestinal schistosomiasis: review. *J Adv Res*. 2013;4(5):445–452. doi:10.1016/j.jare.2012.12.001

69. O'Brien JG, Chennubhotla SA, Chennubhotla RV. Treatment of edema. *Am Fam Physician*. 2005;71(11):2111–2117.

70. D'Mello SR, Das SK, Das NG. Polymeric nanoparticles for small-molecule drugs: biodegradation of polymers and fabrication of nanoparticles. In: *Drug Delivery Nanoparticles Formulation and Characterization*. CRC Press; 2016:36–54.

71. Silva MP, de Oliveira RN, Mengarda AC, et al. Antiparasitic activity of nerolidol in a mouse model of schistosomiasis. *Int J Antimicrob Agents*. 2017;50(3):467–472. doi:10.1016/j.ijantimicag.2017.06.005

72. Guimaraes MA, de Oliveira RN, de Almeida RL, et al. Epiisopilosine alkaloid has activity against Schistosoma mansoni in mice without acute toxicity. *PLoS One*. 2018;13(5):e0196667. doi:10.1371/journal.pone.0196667

73. Adler CE. Dissecting the schistosome cloak. *Elife*. 2018;7. doi:10.7554/eLife.36813

74. Escobedo G, Roberts CW, Carrero JC, Morales-Montor J. Parasite regulation by host hormones: an old mechanism of host exploitation? *Trends Parasitol*. 2005;21(12):588–593. doi:10.1016/j.pt.2005.09.013

75. de Mendonca RL, Escriva H, Bouton D, Laudet V, Pierce RJ. Hormones and nuclear receptors in schistosome development. *Parasitol Today*. 2000;16(6):233–240. doi:10.1016/S0169-4758(00)01641-0

76. AboSheishaa GA. Evaluation of poly lactide-co-glycolide acid [PLGA] nanoparticles loaded with praziquantel in treatment of experimental murine Schistosomiasis mansoni. *EVMSPJ*. 2019;15(1):149–162.

77. Lima TC, Lucarini R, Luz PP, et al. In vitro schistosomicidal activity of the lignan (−)-6, 6′-dinitrohinokinin (DNHK) loaded into poly (lactic-co-glycolic acid) nanoparticles against Schistosoma mansoni. *Pharm Biol*. 2017;55(1):2270–2276. doi:10.1080/13880209.2017.1405996

78. Luz PP, Magalhães LG, Pereira AC, Cunha WR, Rodrigues V. Andrade e Silva ML. Curcumin-loaded into PLGA nanoparticles. *Parasitol Res*. 2012;110(2):593–598. doi:10.1007/s00436-011-2527-9

79. El-Beshbishi SN, Saleh NE, Abd el-Mageed SA, et al. Effect of omega-3 fatty acids administered as monotherapy or combined with artemether on experimental Schistosoma mansoni infection. *Acta Trop*. 2019;194:62–68. doi:10.1016/j.actatropica.2019.02.027

80. Mainardes RM, Chaud MV, Gremião MPD, Evangelista RC. Development of praziquantel-loaded PLGA nanoparticles and evaluation of intestinal permeation by the everted gut sac model. *J Nanosci Nanotechnol*. 2006;6(9–10):3057–3061. doi:10.1166/jnn.2006.487

81. Mokbel KE-DM, Baiuomy IR, Sabry AE-HA, Mohammed MM, El-Dardiry MA. In vivo assessment of the antischistosomal activity of curcumin loaded nanoparticles versus praziquantel in the treatment of Schistosoma mansoni. *Sci Rep*. 2020;10(1):1–9. doi:10.1038/s41598-020-72901-y